IRANIAN JOURNAL OF CATALYSIS

Fe₃O₄-chitosan nanoparticles as a robust magnetic catalyst for efficient synthesis of 5-substituted hydantoins using zinc cyanide

Javad Safari*, Leila Javadian

Laboratory of Organic Compound Research, Department of Organic Chemistry, College of Chemistry, University of Kashan, P.O. Box: 87317-51167 Kashan, I.R. Iran.

ABSTRACT

In this paper, Fe₃O₄-chitosan nanoparticles were prepared by the immobilization of chitosan on the surface of Fe₃O₄ nanoparticles. Then, the 5-substituted hydantoins were synthesized from the condensation of aldehyde derivatives, ammonium carbonate and zinc cyanide as a well-known cyanating agent by the magnetic Fe₃O₄-chitosan nanoparticles under neat conditions. Fe₃O₄-Chitosan nanocatalyst as a renewable hybrid catalyst was easily recovered by an external magnet and reused for 4 times without obvious drop in its catalytic activity. The purpose of this research was to provide an easy method for the synthesis of 5-substituted hydantoins in high yields and short reaction times by a robust and magnetic recoverable catalyst.

Keywords: Fe₃O₄-chitosan, Magnetic catalyst, Hydantoin, Zinc cyanide.

1. Introduction

Nowadays, the development of new methods to reduce pollution in organic reactions has attracted significant attention. In this regard, heterogeneous catalytic systems have been emerged as an effective method to decrease waste production. For this reason, catalysts have been immobilized on various supports. Magnetic iron oxide nanoparticles (Fe₃O₄ MNPs) are very important kind of magnetic materials which were utilized in many fields such as materials science, biology, medicine and physics due to their multi-functional properties such as low toxicity, small size and superparamagnetism, etc [1–6]. The combination of organic and inorganic materials in a particle at the nano-sized level has been rising as a useful material because of the great potential usage in the areas of catalysts. Immobilizing catalysts on the surface of Fe₃O₄ MNPs provides a simple separation of the magnetic catalyst without the need for centrifugation, filtration, or other tedious workup methods [7,8]. Magnetic Fe₃O₄ nanoparticles have been extensively used as catalysts or catalyst supports in different organic transformations with a high level of activity [9–15]. A number of materials have been verified for functionalization and modification of the surface of Fe₃O₄ MNPs [16–21].

Among these compounds, chitosan is one of the most abundant biopolymers in nature that be used to modify the magnetic Fe₃O₄MNPs. It is a natural polymer with many significant biological (biocompatibility, biodegradability, non-toxicity and antibacterial) and chemical properties (hydrogel, polycationic, hydrophilicity and reactive groups) [22–24]. Chitosan is a copolymer of glucosamine and *N*-acetyl-*d*-glucosamine linked together by β (1→4) glycosidic bonds [25–27]. Chitosan can activate the electrophilic and nucleophilic components by lone pairs and hydrogen bonding because of containing reactive hydroxyl and amino functional groups. These requirements exist in the reaction of aldehyde with ammonium carbonate and cyanide for the synthesis of hydantoin derivatives.

Hydantoins are common 5-memberrings that have demonstrated a number of pharmaceutically active compounds including antidiabetic [28], anti-muscarinic [29], anti-viral [30], antitumor [31], anticonvulsant [32], antiandrogenic [33] and antiepileptic [34] activities. The importance of hydantoin derivatives have resulted in the development of efficient methods to synthesis of these well-known molecules. The main pathway to prepare 5- or 5,5-disubstituted hydantoins is the condensation of carbonyl compound, ammonium carbonate and toxic potassium cyanide, known as Bucherer-Bergs reaction. The classical reaction for synthesis of hydantoin derivatives involves alkali metal

*Corresponding author emails: safari_jav@yahoo.com
Tel: +98 31 5591 2320; Fax: +98 31 5551 1121

cyanides [35]. One of the greatest needs in Bucherer-Bergs reaction is a safe cyanating agent compared to KCN that eliminates or reduces the need to toxic cyanide source. In search of efficient synthesis in an environmental method, a number of modifications have been reported using different cyanating agents such as TMSCN, ethyl cyanoformate, MeCOCN and Bu_3SnCN in the presence of different catalysts have been described [36–39]. But, there is no report about using other cyanating agent in the literature for the synthesis of hydantoin derivatives. Although trimethylsilyl cyanide is used as a commonly cyanide source, it is expensive, and moisture sensitive. So, the major disadvantages of reported techniques are the use of expensive reagents, strong acidic conditions, extended reaction time and the generation of toxic waste. In view of these difficulties, it is desirable to investigate for a cheap and safe reagent compared to KCN for the synthesis of hydantoin derivatives. $Zn(CN)_2$ has been used as a cyanide source in the synthesis of α-aminonitriles [40], phthalonitriles [41], benzonitriles [42], 2-cyanoisonicotinamide [43] and in cycloaddition reactions [44]. Advantage of using zinc cyanide is related to its lower toxicity compared to other cyanide sources. Therefore, we reported an efficient method for the synthesis of hydantoin derivatives using $Zn(CN)_2$ as a well-known non-toxic cyanating agent in the presence of Fe_3O_4-chitosan nanoparticles as heterogeneous magnetic catalyst.

2. Experimental

2.1. Materials and apparatus

Chemical reagents in high purity were purchased from the Merck Chemical Company. Melting points were determined in open capillaries using an Electrothermal Mk3 apparatus and are uncorrected. ^{1}HNMR spectra were recorded with a Bruker DRX-400 spectrometer at 400 and 100 MHz respectively. NMR spectra were reported as parts per million (ppm) downfield. The abbreviations used are: singlet (s), doublet (d), triplet (t) and multiplet (m). FT-IR spectra were obtained with potassium bromide pellets in the range 400–4000 cm^{-1} with a Perkin–Elmer 550 spectrometer. Elemental composition of mentioned magnetic nanoparticles was investigated by EDAX spectroscopy. The XRD patterns of samples were obtained with a Philips Xpert X-ray powder diffractometer (CuK radiation, k= 0.154056 nm). The nanoparticles morphology were examined by SEM (Hitachi S4160 scanning electron microscope) and the TEM images were recorded using a Ziess EM10C transmission electron microscope operated at a 80 kV accelerating voltage. Sonication was performed in a Shanghai Branson-BUG40-06 ultrasonic cleaner.

2.2. Preparation of magnetic Fe_3O_4-chitosan catalyst

Fe_3O_4-chitosan nanoparticles were prepared by a simple method. Firstly, Fe_3O_4 nanoparticles were prepared by chemical co-precipitation described in the literature [45]. In order to prepare modified Fe_3O_4–chitosan MNPs, the Fe_3O_4 nanoparticles (0.5 g) were initially dispersed in 50 mL of distilled water for about 30 min under ultrasound irradiation. In second step, 0.25 g of chitosan was dissolved in 2.0 wt% acetic acid solution (70 mL) and was slowly added to the disperse Fe_3O_4 NPs in a drop-wise manner under continuous mechanical stirring at 50°C. After vigorous stirring for about 1 h, the Fe_3O_4–chitosan nanoparticles were collected from the reaction mixture through a permanent magnet. Then, the nanocatalyst was washed several times with ethanol. Finally, the products were dried under vacuum at 60°C for 2 h.

2.3. General procedure for the synthesis of 5-substituted hydantoin using Fe_3O_4-chitosan nanocatalyst

Into a 25 mL round-bottomed flask, a mixture of zinc cyanide (1 mmol), water/ethanol/acetic acid (1:1:1), aldehyde (1 mmol) and Fe_3O_4-chitosan (20 mg) were charged. Afterward, ammonium carbonate (5 mmol) was added to the reaction mixture and heated at 60°C for the appropriate time. The reaction progress was monitored by TLC (petroleum ether: ethyl acetate= 2:1 v/v). After completion of the reaction, the reaction mixture was allowed to cool to room temperature. The catalyst was removed by an external magnet, was washed with diethyl ether three times and finally was dried. So, the magnetic catalyst was recycled and subjected to a second run of the reaction. Then, the resulted solution was neutralized with diluted hydrochloric acid. Pure products were obtained after recrystallization from ethanol and the corresponding products were characterized by comparison of their physical and spectral data with those previously reported. The spectral data for the selected products are provided below.

Selected spectral data

5-(2,4-dichlorophenyl)-imidazolidine-2,4-dione **(Table 3, entry 4)**:

White crystal. m.p.= 182-183˚C. ^{1}HNMR (Acetone-d_6, 400 MHz): δ= 5.65 (s, 1H, CH), 7.370 (s, 1H, NH), 7.44-7.47 (dd, J_1= 8.6 Hz, J_2= 2 Hz, 1H, Ar-H), 7.51-7.53 (d, J= 8.4 Hz, 1H, Ar-H), 7.582-7.587 (d, J= 2 Hz, 1H, Ar-H), 10.11 (s, 1H, NH) ppm. IR (KBr): $\bar{v}$ = 3388 (NH), 3247 (NH), 2926 (C-H), 1730 (C=O), 1419 (N-H) cm^{-1}. UV (CH$_3$OH): λ_{max} =222 nm.

*5-(5-methyl-2-furyl)-imidazolidine-2,4-dione (**Table 3, entry** 7):*

White crystal. m.p.= 135-137˚C. ^{1}HNMR (Acetone-d_6, 400 MHz): δ= 2.22 (s, 3H, CH), 5.23 (s, 1H, CH), 6.00 (d, 1H, *J*= 3.5 Hz), 6.53 (d, 1H, *J*= 3.5 Hz), 7.35 (s, 1H, N$_1$H), 9.79 (s, 1H, N$_3$H) ppm. IR (KBr): $\bar{v}$ = 3355 (NH, s), 3207 (NH, s), 2923 (CH), 1765 (C=O), 1721 (C=O), 1414 (N-H, b) cm^{-1}. UV (CH$_3$OH): λ$_{max}$= 260, 340 nm.

*5,5'-(1,4-phenylene)bis(imidazolidine-2,4-dione) (**Table 3, entry** 8):*

Pale yellow powder. m.p.>300˚C. ^{1}HNMR (DMSO-d_6, 400 MHz,): δ= 5.16 (s, 2H, CH), 7.33 (s, 4H), 8.41 (s, 2H, N$_1$-H), 10.75 (s, 2H, N$_3$-H); IR (KBr): $\bar{v}$ = 3363 (NH, s), 3123 (=CH), 2926 (CH), 1700 (C=O), 1688 (C=O), 1576 (C=C), 1500 (NH, b) cm^{-1}. UV (CH$_3$OH): λ$_{max}$ = 273 nm.

3. Results and Discussion

3.1. Characterization of magnetic catalyst

The structure of nanoparticles was characterized by various methods including FT-IR spectroscopy, XRD, TEM, SEM, and EDX.

The FT-IR spectra of Fe$_3$O$_4$ nanoparticles demonstrated characterization peaks for Fe–O–Fe at 570 cm^{-1} and O–H groups at 3423 cm^{-1} (Fig. 1a). Fig. 1b shows the absorption bands in chitosan: the (C-O) of primary alcoholic group at 1224 cm^{-1}, the (C-H) at 2874 and 2940 cm^{-1} and also the (NH) at 3435 and 1653 cm^{-1}. For Fe$_3$O$_4$-chitosan composite, additional peaks were observed for C-H and C-O, which indicates successful immobilization of chitosan

on the surface of Fe$_3$O$_4$ nanoparticles (Fig. 1c). The presence of chitosan molecule shifted the vibration of Fe$_3$O$_4$ MNPs. The bands shift of N-H bending vibration from 1653 to 1633 cm^{-1} and Fe-O stretching vibration from 570 to 576 cm^{-1} are significant. Also, a peak at around 2924 cm^{-1} was attributed to C-H stretching band of chitosan in Fig. 1c. The peak at 3430 cm^{-1} was corresponded to the amino groups of chitosan, which is overlapped by the O-H groups stretching vibration of Fe$_3$O$_4$.

The morphology and particle size of magnetic nanoparticles were confirmed by SEM and TEM images (Fig. 2).
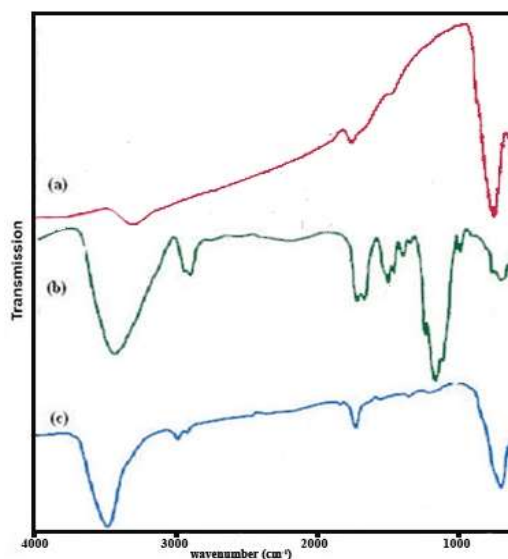
Fig. 1. FT-IR spectra of pure Fe$_3$O$_4$ NPs (a), chitosan (b) and Fe$_3$O$_4$-chitosan (c).
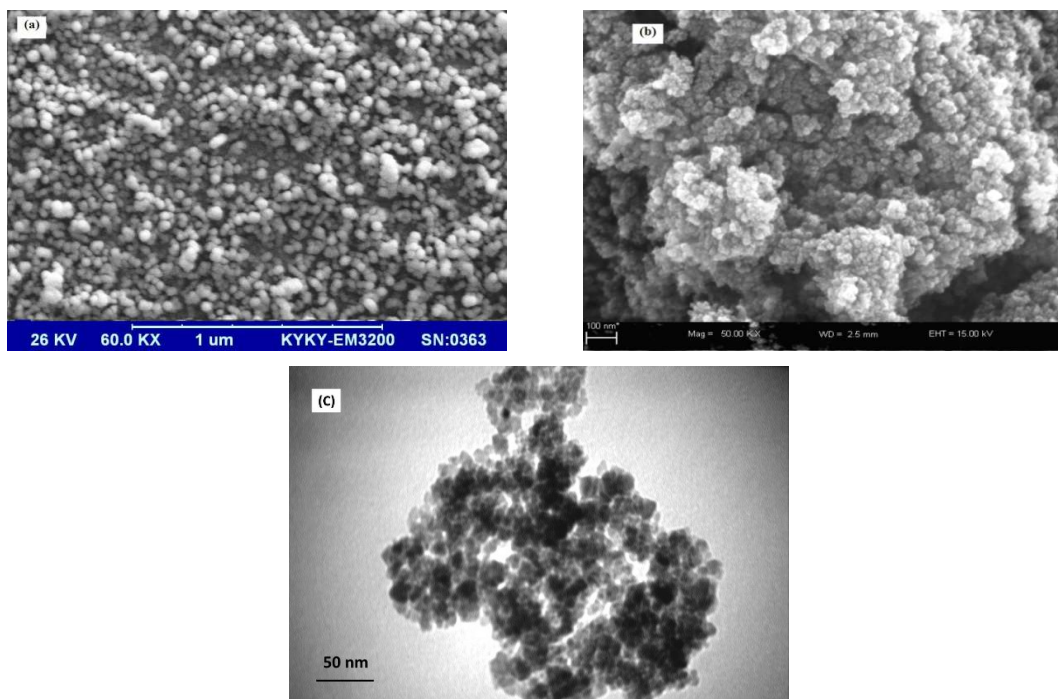
Fig. 2. The SEM images of pure Fe$_3$O$_4$ (a), Fe$_3$O$_4$-CS NPs (b) and the TEM image of Fe$_3$O$_4$-CS NPs (c).

The SEM image of the Fe_3O_4 nanoparticles exhibits that Fe_3O_4 nanoparticles have smooth surfaces without any coagulation. There are two kinds of the surface morphology for Fe_3O_4-chitosan MNPs in Fig. 2b. On the basis of the TEM image, Fe_3O_4-chitosan nanoparticles indicated spherical shape and smooth surface. (Fig. 2c) It shows two regions with different electron densities that it can be confirms a layer of chitosan on the surface of Fe_3O_4 with different phase. An electron dense region corresponds to Fe_3O_4 and a more translucent region surrounding corresponds to chitosan.

In addition, the presence of chitosan on the surface of Fe_3O_4 nanoparticles was verified by the appearance of N and O elements in EDX analysis. Based on Fig. 3, the amount of Fe, O, N and C on the surface of Fe_3O_4 nanoparticles was around 74.6, 21.94, 0.52 and 2.94% by weight.

Fig. 4 shows the XRD pattern of Fe_3O_4 and Fe_3O_4-chitosan nanoparticles. The data for the Fe_3O_4 nanoparticles corresponded to the presence of the cubic inverse spinel structure of Fe_3O_4. The XRD pattern of the Fe_3O_4-chitosan was in good agreement with of Fe_3O_4 phase, indicating the chitosan did not induce any phase change, except for a broad peak around $2\theta = 15$-$20°$ corresponding to amorphous phase of chitosan. Increase the noise and change in peaks intensity verify the anchoring of chitosan on the surface of Fe_3O_4 MNPs. From the XRD pattern, the crystal size of 15 nm for Fe_3O_4 and 19 nm for Fe_3O_4-chitosan composite could be estimated.

The magnetic properties of Fe_3O_4 and Fe_3O_4-chitosan nanoparticles were evaluated by VSM at room temperature (Fig. 5). The results of VSM showed that the saturation magnetization of the pure Fe_3O_4 nanoparticles was about 55.69 emu/g. The saturation magnetization value reduced to 50.27 emu/g after surface coating with chitosan polymer. The decrease of the saturation magnetization of Fe_3O_4-chitosan MNPs indicates the presence of a diamagnetic layer (chitosan) at the surface of the Fe_3O_4 nanoparticles.

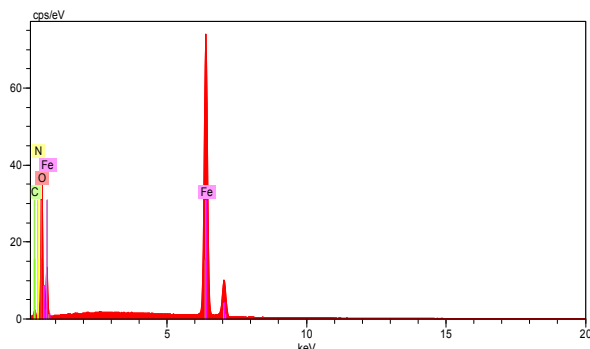All of these observations proved the successful immobilization of chitosan on the surface of the Fe_3O_4 nanoparticles.

3.2. Optimization of reaction conditions

At first, in order to search the importance of $Zn(CN)_2$ as a safe cyanating agent compared to KCN and the catalytic activity of the Fe_3O_4-chitosan MNPs as a magnetic catalyst, the reaction between benzaldehyde, ammonium carbonate $Zn(CN)_2$ and Fe_3O_4-chitosan MNPs was carried out as a model reaction at 60°C. But we did not observe the formation of product after 2 h. The current reaction using zinc cyanide afforded desired product in the presence of acetic acid. To explore the effect of solvent, the condensation of benzaldehyde, zinc cyanide and ammonium carbonate and 20 mg of magnetic nanocatalyst was carried out in various solvents (Table 1).
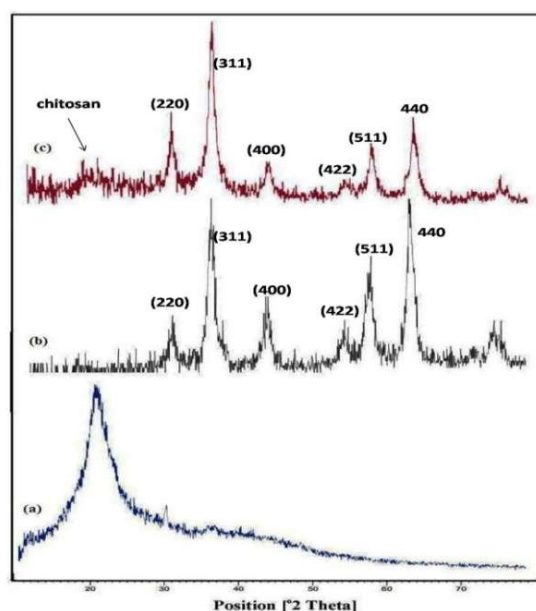

Fig. 4. The XRD pattern of chitosan (a), Fe_3O_4 (b) and Fe_3O_4-chitosan NPs (c).
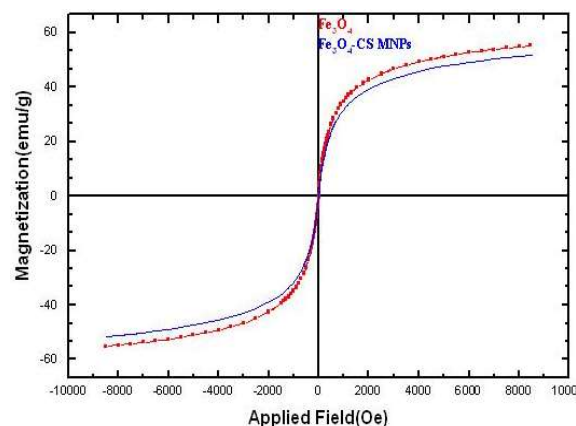

Fig. 3. The energy dispersive X-ray (EDX) of Fe_3O_4-chitosan NPs.

Fig. 5. Magnetization versus of Fe_3O_4 and Fe_3O_4-chitosan nanoparticles.

Table 1. Effect of various solvents on the formation of 4a.[a]

Entry	Solvent	Yield (%)	Time (min)
1	EtOH/H_2O	-	150
2	H_2O/AcOH	93	32
3	DMSO/AcOH	85	27
4	H_2O/EtOH/AcOH	97	13
5	CH_3CN/AcOH	90	34
6	$CHCl_3$/AcOH	73	54

[a]Reaction conditions: Aldehyde (1 mmol), ammonium carbonate (5 mmol), $Zn(CN)_2$ (1 mmol) and Fe_3O_4-chitosan (20 mg).

Table 2. The effect of catalyst amount on the synthesis of hydantoin derivatives.[a]

| Entry	Catalyst amount (mg)	Time (min)	Yield (%)
1	-	50	32
2	10	35	85
3	15	28	93
4	20	13	97
5	25	17	97

[a]Reaction conditions: Aldehyde (1 mmol), ammonium carbonate (5 mmol), $Zn(CN)_2$ (1 mmol) and water/Ethanol/AcOH (1:1:1).

The results show that water/ethanol is more efficient among the various solvents studied. Improved yield and the enhanced reaction rate are the results obtained in the presence of water/ethanol/acetic acid (1:1:1).

The effect of amount of nanocatalyst was surveyed on the synthesis of the 5-phenylhydantoin by varying the amount of magnetic catalyst (Table 2). We found that in the absence of catalyst, the corresponding product was afforded in low yield. The reaction yields were significantly affected by the amount of magnetic catalyst and the yields enhanced with an increase in the amount of magnetic catalyst in shorter reaction time. The usage of higher than 20 mg of magnetic catalyst did not increase the yields.

Having the optimized reaction conditions, we then applied this new method for the synthesis of other 5-substituted hydantoins to ascertain the substrate scope of the reaction. So, a variety of aldehydes (aromatic, heteroaromatic or aliphatic) were condensed with ammonium carbonate in the presence of zinc cyanide and Fe_3O_4-chitosan MNPs to produce hydantoin derivatives (Scheme 1).

As listed in Table 3, the Fe_3O_4-chitosan-catalyzed reaction with aromatic aldehydes containing groups such as chloro, methyl and methoxy afforded the desired products in excellent yields. The results showed that heteroaromatic aldehydes (furfural, 5-methylfurfural and pyridine-3-carbaldehyde) as well as aromatic aldehydes afforded excellent yields. It should be noted that terephthaldehyde as an aromatic

dialdehyde showed the lowest yield among the aldehydes evaluated under the same reaction conditions. In addition, aliphatic aldehydes worked well under these conditions. These reactions proceeded with high yields without any undesired side product and $Zn(CN)_2$ reacted in the preferred way.
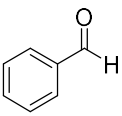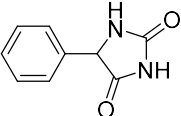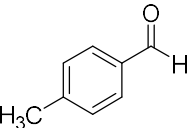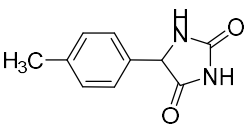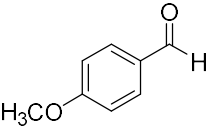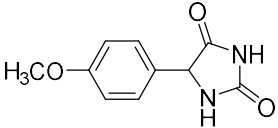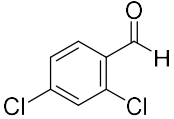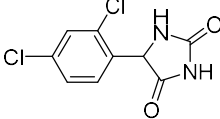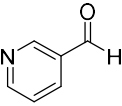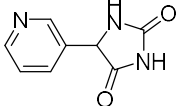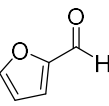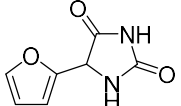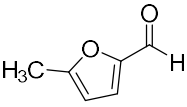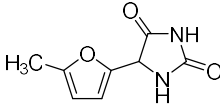
Based on our observation in the current work, a preferable reaction mechanism is suggested. In the first step, the hydroxyl groups of chitosan on the surface of the Fe_3O_4 NPs can activate the carbonyl group of the aldehyde through hydrogen bonding and increases the electrophilic character of the carbonyl groups. The addition of the ammonia to activate the carbonyl group gives rise to imine. Then, α-aminonitrile is formed from the reaction of imine with anion cyanide. This way is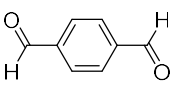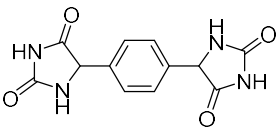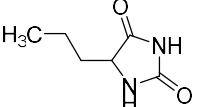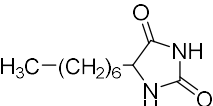 followed by the nucleophilic addition of α-aminonitrile with carbon dioxide,which undergoes an intramolecular ring closing to 5-imino-oxazolidin-2-one. Finally, hydantoin is produced via an isocyanate intermediate (Scheme 2).

3.3. Reusability of the catalyst

The reusability of the magnetic catalyst was tested for the synthesis of 5-phenyl hydantoin under optimized conditions. After completion of the reaction, the catalyst was removed from the reaction mixture and the recovered nanocatalyst was washed several times with diethyl ether, and reused for subsequent reactions four times without obvious decreasing in catalytic activity. The yields was 96% at first run and 96, 95, 94 and 90 % for four subsequent reactions respectively.
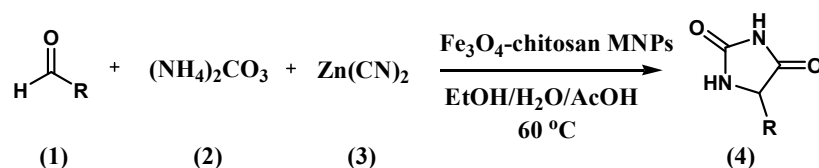
Scheme 1. Synthesis of 5-substituted hydantoins catalyzed by Fe_3O_4-chitosan MNPs.

Table 3. Preparation of 5-substituted hydantoins in the presence of Fe_3O_4-chitosan MNPs.[a]

Entry	Substrate	Product	Time (min)	Yield (%)	m.p.(°C) Found	m.p.(°C) Reported	Ref.
1			13	97	182-184	183-184	[49]
2			16	89	183-185	183-184	[50]
3			17	95	193-197	190-192	[51]
4			19	90	182-183	179-181	[46]
5			12	96	310-313	308-309	[52]
6			19	89	149-151	147	[50]
7			20	88	135-137	135-139	[47]
8			25	80	>300	>300	[48]
9	$OHC-(CH_2)_2CH_3$		23	85	132-135	136-137	[53]
10	$OHC-(CH_2)_6CH_3$		23	84	144-147	142-143	[54]

[a]Reaction conditions: Aldehyde (1 mmol), ammonium carbonate (5 mmol), $Zn(CN)_2$ (1 mmol), water/Ethanol/AcOH (1:1:1) and Fe_3O_4-chitosan (20 mg).
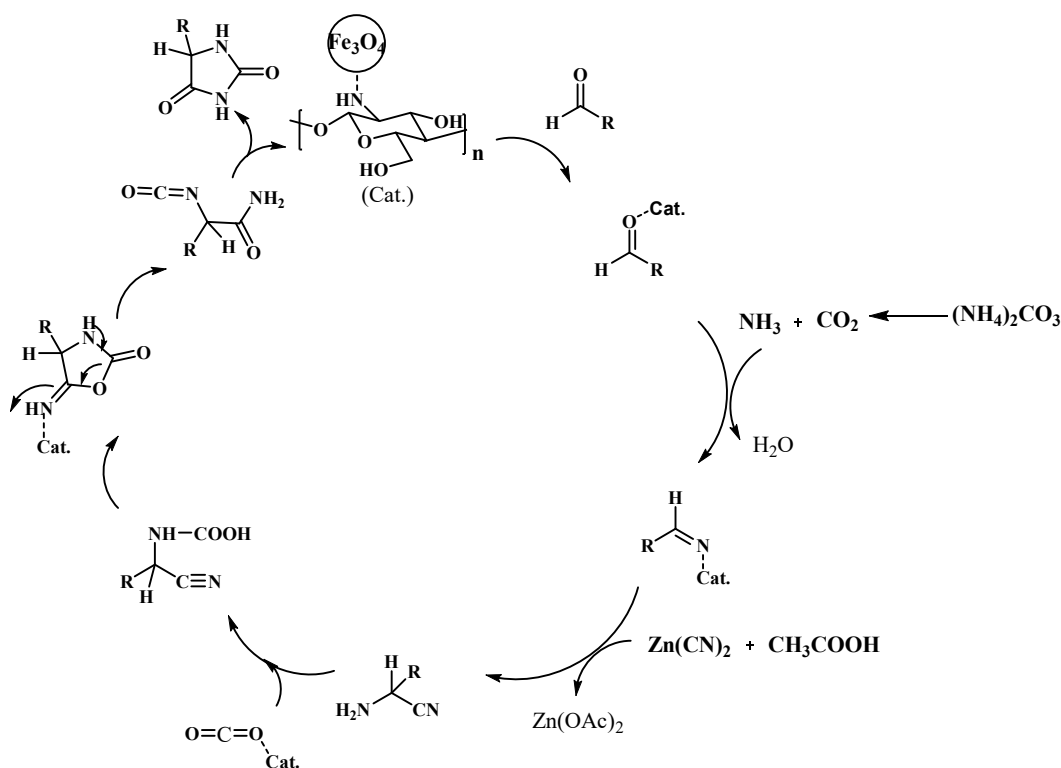
Scheme 2. Plausible mechanism for the synthesis of 5-substituted hydantoins using Fe_3O_4-chitosan as a magnetic catalyst.

4. Conclusions

In conclusion, 5-substituted hydantoins were obtained with high purity in an efficient manner using the Fe_3O_4-chitosan MNPs as a magnetic nanocatalyst and $Zn(CN)_2$ as a cyanide source without formation of toxic waste. Totally, the simplicity of the experimental procedure, simple work-up, high yield, avoidance of toxic solvents, the use of non-toxic and readily available cyanide source were the advantages of the present protocol in the synthesis of 5-substituted hydantoins. Also, no harmful by-products were produced during reaction work-up.

Acknowledgements

References

[1] J. Qu, G. Liu, Y. Wang, R. Hong, Adv. Powder Technol. 21 (2010) 461-467.

[2] G. Li, Y. Jiang, K. Huang, P. Ding, J. Chen, J. Alloys Compd. 466 (2008) 451-456.

[3] Y. Wu, J. Guo, W.L. Yang, C.C. Wang, S.K. Fu, Polymer 47 (2006) 5287-5294.

[4] P. Wunderbaldinger, L. Josephson, R. Weissleder, Bioconjugate Chem. 13 (2002) 264-268.

[5] W. Wang, L. Deng, Z.H. Peng, X. Xiao, Enzym. Microb. Technol. 40 (2007) 255-261.

[6] H. Gu, K. Xu, C. Xu, B. Xu, Chem. Commun (2006) 941-949.

[7] L. Zhou, C. Gao, W. Xu, Langmuir 26 (2010) 11217-11225.

[8] B. Karimi, F. Mansouri, H. Vali, Green Chem. 16 (2014) 2578-2596.

[9] T. Zeng, L. Yang, R. Hudson, G. Song, A.R. Moores, C.J. Li, Org. Lett. 13 (2011) 442-445.

[10] C. Park, H.J. Lee, H.S. Jung, M. Kim, H.J. Kim, K.H. Park, H. Song, Chem. Cat. Chem. 3 (2011) 755-760.

[11] S. Wittmann, A. Schatz, R.N. Grass, W.J. Stark, O. Reiser, Angew. Chem. Int. Ed. 49 (2010) 1867-1870.

[12] B. Kaboudin, R. Mostafalu, T. Yokomatsu, Green Chem. 15 (2013) 2266-2274.

[13] R.L. Oliveira, P.K. Kiyohara, L.M. Rossi, Green Chem. 12 (2010) 144-149.

[14] L. M. Rossi, F.P. Silva, L.L.R. Vono, P.K. Kiyohara, E.L. Duarte, R. Itri, R. Landers, G. Machado, Green Chem. 9 (2007) 379-385.

[15] Y. Wang, J.K. Lee, J. Mol. Catal. A: Chem. 263 (2007) 163-168.

[16] L. Xu, W. Zhang, Y. Ding, Y. Peng, S. Zhang, W. Yu, Y. Qian, J. Phys. Chem. B 108 (2004) 10859-10862.

[17] R.-Y. Hong, J.-H. Li, S.-Z. Zhang, H.-Z. Li, Y. Zheng, J.-M. Ding, D.-G. Wei, Appl. Surf. Sci. 255 (2009) 3485-3492.

[18] L.Y. Wang, H.Y. Park, S.I.I. Lim, M.J. Schadt, D. Mott, J. Luo, X. Wang, C.J. Zhong, J. Mater. Chem. 18 (2008) 2629-2635.

[19] A. Maleki, N. Ghamari, M. Kamalzare, RSC Adv. 4 (2014) 9416-9423.

[20] L.D. Tran, B.H. Nguyen, N.V. Hieu, H.V. Tran, H.L. Nguyen, P.X. Nguyen, Mater. Sci. Eng. C 31 (2011) 477-485.

[21] H.V. Tran, L.D. Tran, T.N. Nguyen, Mater. Sci. Eng. C 30 (2010) 304-310.

[22] A. Bozkir, O.M. Saka, Drug Deliv. 11 (2004) 107-112.

[23] Y. Chang, D. Chen, J. Colloid Interface Sci. 283 (2005) 446-451.

[24] N.D. Cuong, T.T. Hoa, D.Q. Khieu, T.D. Lam, N.D. Hoa, N. Van Hieuc, J. Alloys Compd. 523 (2012) 120-126.

[25] X. Xue, J. Wang, L. Mei, Z. Wang, K. Qi, B. Yang, Coll. Surf. B Biointerfaces 103 (2013) 107-113.

[26] L. Zhang, X. Zhu, H. Sun, G. Chi, J. Xu, Y. Sun, Curr. Appl. Phys. 10 (2010) 828-833.

[27] Z. Lei, X. Pang, N. Li, L. Lin, Y. Li, J. Mater. Process. Technol. 209 (2009) 3218-3225.

[28] L. Somsak, M.L. Kovacs, E. Toth, L. Osz, Z. Szilagyi, Z. Gyorgydeak, T. Dinya, B. Docsa, P.G. Toth, J. Med. Chem. 44 (2001) 2843-2848.

[29] J.C. Thenmozhiyal, P.T.H. Wong, W.K. Chui, J. Med. Chem. 47 (2004) 1527-1535.

[30] F. Medda, C. Hulme, Tetrahedron Lett. 53 (2012) 5593-5593.

[31] S.K. Agrawal, M. Sathe, A.K. Halve, M.P. Kaushik, Tetrahedron Lett. 53 (2012) 5996-5999.

[32] A. Alizadeh, E. Sheikhi, Tetrahedron Lett. 48 (2007) 4887-4890.

[33] L. Grosse, S. Paquet, P. Caron, L. Fazli, P.S. Rennie, A. Belanger, O. Barbier, Cancer Res. 73 (2013) 6963-6971.

[34] M. Dhanawat, A.G. Banerjee, S.K. Shrivastava, Med. Chem. Res. 21 (2011) 2807-2822.

[35] R.G. Murray, D.M. Whitehead, F. Le Stratb, S.J. Conway, Org. Biomol. Chem. 6 (2008) 988-991.

[36] K. Shen, X.H. Liu, Y.F. Cai, L.L. Lin, X.M. Feng, Chem. Eur. J. 15 (2009) 6008-6014.

[37] J.P. Abell, H. Yamamoto, J. Am. Chem. Soc. 131 (2009) 15118-15119.

[38] F. Cruz-Acosta, A. Santos-Exposito, P. Armas, F. García-Tellado, Chem. Commun. 44 (2009) 6839-6841.

[39] Z.F. Xie, G.L. Li, G. Zhao, J.D. Wang, Synthesis (2009) 2035-2039.

[40] S. Shah, B. Singh, Tetrahedron Lett. 53 (2012) 151-156.

[41] Z. Iqbal, A. Lyubimtsev, M. Hanack, Synlett (2008) 2287-2290.

[42] M. Shevlin, Tetrahedron Lett. 51 (2010) 4833-4836.

[43] Z. Huo, T. Kosugi, Y. Yamamoto, Tetrahedron Lett. 49 (2008) 4369-4371.

[44] M. Alterman, H.O. Andersson, N. Garg, G. Ahlsen, S. Lovgren, B. Classon, U.H. Danielson, I. Kvarnstrom, L. Vrang, T. Unge, B. Samuelsson, A. Hallberg, J. Med. Chem. 42 (1999) 3835-3844.

[45] J. Safari, L. Javadian, RSC Adv. 4 (2014) 48973-48979.

[46] L.M. Werbel, E.F. Elslager, J. Med. Chem. 20 (1977) 1569-1572.

[47] R.H. Divanford, A.Y. Ibrahim, M.M. Joullie, J. Heterocycl. Chem. 15 (1978) 691-786.

[48] S.K. Ahmed, J.-L.G. Etoga, S.A. Patel, R.J. Bridges, C.M. Thompson, Bioorg. Med. Chem. Lett. 21 (2011) 4358-4362.

[49] N.O. Mahmoodi, Z. Khodaee, Arkivoc 2007 (2007) 29-36.

[50] H.R. Henze, R.J. Speer, J. Am. Chem. Soc. 64 (1942) 522-523.

[51] G.A. Pinna, E. Gavinil, G. Cignarellaz, S. Scolastico, P. Fadda, Eur. J. Med. Chem. 30 (1995) 515-520.

[52] V.M. Viscontini, H. Raschig, Helv. Chim. Acta. 42 (1959) 570-573.

[53] E.J. Mcmullen, H.R. Henze, B.W. Wyatt, J. Am. Chem. Soc. 76 (1954) 5646-5650.

[54] T. Johnson, J. Am. Chem. Soc. 61 (1939) 2485-2487.